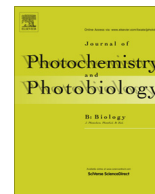




Contents lists available at ScienceDirect

Journal of Photochemistry and Photobiology B: Biology

journal homepage: www.elsevier.com/locate/jphotobiol

Synthesis, characterization, DNA-binding studies and acetylcholinesterase inhibition activity of new 3-formyl chromone derivatives

Mehtab Parveen^{a,*}, Ali Mohammed Malla^a, Zahid Yaseen^b, Akhtar Ali^a, Mahboob Alam^a^a Department of Chemistry, Aligarh Muslim University, Aligarh 202002, India^b Department of Civil Engineering, Islamic University of Science and Technology, Kashmir 192122, India

ARTICLE INFO

Article history:

Received 25 July 2013

Received in revised form 29 October 2013

Accepted 18 November 2013

Available online 26 November 2013

Keywords:

Synthesis

Chromone

Fluorescence

DNA binding

Acetylcholinesterase inhibition

ABSTRACT

A series of new substituted 3-formyl chromone derivatives (**4–6**) were synthesized by one step reaction methodology by Knoevenagel condensation, structurally similar to known bisintercalators. The new compounds were characterized by IR, ¹H NMR, ¹³C NMR, MS and analytical data. The in vitro DNA binding profile of compounds (**4–6**) was carried out by absorption, fluorescence and viscosity measurements. It was found that synthesized compounds, especially compound **6** (evident from binding constant value) bind strongly with calf thymus DNA, presumably via an intercalation mode. Additionally, molecular docking studies of compounds (**4–6**) were carried out with B-DNA (PDBID: 1BNA) which revealed that partial intercalative mode of mechanism is operational in synthesized compounds (**4–6**) with CT-DNA. The binding constants evaluated from fluorescence spectroscopy of compounds with CT-DNA follows the order compound **6** > compound **5** > compound **4**. All the compounds (**4–6**) were screened for acetylcholinesterase inhibition assay. It can be inferred from data, that compound (**6**) showed potent AChE inhibition having IC₅₀ = 0.27 μM, almost in vicinity to reference drug Tacrine (IC₅₀ = 0.19 μM).

© 2013 Elsevier B.V. All rights reserved.

1. Introduction

Chromones are a group of naturally occurring compounds that is ubiquitous in nature especially in plants [1]. They are oxygen-containing heterocyclic compounds with a benzo-annelated γ -pyrone ring, with the parent compound being chromone (4H-chromen-4-one, 4H-1-benzopyran-4-one) [2]. Besides forming the basic nucleus of an entire class of natural products (i.e., flavones) [3,4], the chromone scaffold forms the key component of a large number of bioactive molecules of either natural or synthetic origin, possessing anti-inflammatory, antitumoral, and antimicrobial activities [5]. The benzo- γ -pyrone nucleus of chromone moiety has been reported to exhibit enzymatic inhibition properties toward different systems such as oxidoreductases, kinases, tyrosinases, and cyclooxygenases [6]. The relevance of these types of heterocyclic compound as monoamine oxidase inhibitors (MAOIs) has been recently reported in literature [7].

In recent years, 3-formyl-chromones have attracted considerable attention as highly reactive compound, which can serve as the valuable moiety for incorporation in heterocycles with useful properties due to the presence of a keto function at C-4, a conjugated second carbonyl group at C-3, and above all, possess a highly

polarized C₂–C₃ π -bond [8]. 3-Heteryl-substituted chromones are known to exhibit wide range of biological activities. The substitution pattern of the chromone scaffolds determines their different biological effects. Known effects of these types of compounds are antioxidant [9], antiviral [10], antibacterial activities [11] or kinase inhibition [12]. Hence, chromones can be considered as privileged structures, defined as “a single molecular framework able to provide ligands for diverse receptors” [13]. Derivatives of 3-formyl chromone are useful synthetic building blocks in both organic and medicinal chemistry [14]. Introduction of an electron-withdrawing group at position 3 of chromones radically changes the reactivity of the pyrone ring toward nucleophilic reagents and opens up a broad synthetic scope of this important oxygen-containing heterocyclic system. Being essentially gem-activated alkenes, 3-substituted chromones exhibit a variety of properties and can undergo additional transformations through opening of the γ -pyrone ring [15,16]. The photophysical behavior of 3-hydroxychromones has been carefully studied and efforts have been made to develop derivatives with improved and exceptional fluorescent properties. Due to their characteristic fluorescence behavior, 3-hydroxychromone derivatives have been used as biosensors, hydrogen bonding sensors and as fluorescent probes for dipotential (Ψ D) measurements in lipid bilayers [17–20]. They have also been used for studies of DNA interactions and as photochemical dyes for protein labeling and apoptosis [21–23].

* Corresponding author. Tel.: +91 9897179498.

E-mail address: mehtab.organic2009@gmail.com (M. Parveen).

Metal complexes have been widely investigated as cleaving agents of nucleic acids and are found to be reasonably efficient [24,25], but their use in pharmacy is restricted because of serious issues over their stability and toxicity, that limits the practical usage of these compounds [26,27]. To overcome these limitations, Gobel and co-workers [28,29] put forward the concept of 'metal-free cleaving agents' which are being applied to active phosphodiesterases like 'nucleic acid mimic' and RNA. The structure of the chromone ring meets the requirements for the terminal moiety of bisintercalators. The association of such two almost planar unsaturated systems with the unsaturated linker may guide to the formation of molecules which exhibit specific biological properties, e.g., antitumor activity and are capable of binding to DNA via a bisintercalative binding mode (simultaneous insertion of two planar systems between the adjacent base-pairs according to a neighbor exclusion principle) [30]. Bisintercalators constitute a versatile and very promising group of compounds extensively studied by many research groups worldwide. Lots of them turned out to be potent anticancer drugs e.g., elinafide, bisnaphthalimide which progressed to clinical trials against solid tumors [31].

Encouraged by the above results, herein, we report the synthesis of substituted 3-formyl chromone derivatives by Knoevenagel Condensation, containing chroman–chromen rings tethered at the 3, 3' position by ylidene methyl moiety and behave as metal free DNA binding agents. The presence of NH₂ and CO groups in the molecules can cooperatively participate in the interaction with DNA via hydrogen bonding. A computer aided molecular docking study was carried out to validate the specific binding mode of the synthesized compounds.

2. Experimental

2.1. Material and methods

Melting points were determined on a Kofler apparatus and are uncorrected. Elemental analysis (C, H, N) were conducted using Carlo Erba analyzer model 1108. The IR spectra were recorded with Shimadzu IR-408 Perkin-Elmer 1800 (FTIR) and its values are given in cm⁻¹. ¹H NMR and ¹³C NMR spectra were run in DMSO-d₆ on a Bruker Advance-II 400 MHz instrument with TMS as internal standard. Chemical shifts are reported in ppm (δ) relative to the TMS. Mass spectra were recorded on a JEOL D-300 mass spectrometer. Thin layer chromatography (TLC) plates were coated with silica gel G and exposed to iodine vapors to check the homogeneity as well as the progress of reaction. Sodium sulfate (anhydrous) was used as a drying agent. The calf Thymus DNA was purchased from Bangalore Genei (India). All the reagents were purchased from Sigma-Aldrich Chemicals Pvt. Ltd. which were of analytical grade and used without further purification.

2.2. General procedure for the synthesis of compounds (4–6)

The appropriate substituted 3-formylchromones (1–3) and 4-chromanone (2 mmol) each, were dissolved in 25 mL of absolute ethanol. To this solution catalytic amount of piperidine was added and the reaction mixture was stirred at 140 °C for 2–3 h. The completion of the reaction was monitored by TLC. After completion of the reaction as evident from TLC, the precipitate formed was filtered, thoroughly washed with 5% HCL solution and then with (2 × 100 mL) water, dried and crystallized from CHCl₃–MeOH to afford pure products (4–6) (Scheme 1).

2.2.1. 3-(4'-Oxo-chroman-3'-ylidene methyl)-chromen-4-one (4)

It was crystallized from CHCl₃–MeOH as brick red color solid; Yield: 84%; m.p 145–47 °C. Anal. Calc. for C₁₉H₁₂O₄: C, 74.99; H,

3.97; found: C, 75.0; H, 3.96; IR (KBr) cm⁻¹: 1650, 1591, 1496, 1416, 1373, 1250, 1154. ¹H NMR (400 MHz, DMSO-d₆, δ, ppm): 7.09–8.24 (m, 8H, Ar–H); 6.02 (s, 1H, Exocyclic vinylic-H), 5.98 (s, 1H, vinylic-_γ-pyrone), 4.87 (s, 2H, O–CH₂). ¹³C NMR (400 MHz, DMSO-d₆, δ, ppm): 185.37 (C=O), 183.24 (C=O), 158.21, 154.47, 153.55, 135.72, 131.85, 129.59, 128.94, 126.26, 125.82, 124.45, 123.2, 122.12, 115.16, 114.68 (Chroman/chromen ring), 68.23 (O–CH₂). MS (ES+) m/z: 303.

2.2.2. 6-Bromo-3-(4'-oxo-chroman-3'-ylidene methyl)-chromen-4-one (5)

It was crystallized from CHCl₃–MeOH as brown color solid; Yield: 73%; m.p 188–90 °C. Anal. Calc. for C₁₉H₁₁BrO₄: C, 59.55; H, 2.89; Br, 20.85; found: C, 59.54; H, 2.88; Br, 20.85; IR (KBr) cm⁻¹: 1651, 1595, 1491, 1370, 1298, 1246, 1174. ¹H NMR (400 MHz, DMSO-d₆, δ, ppm): 7.15–8.11 (m, 7H, Ar–H), 6.13 (s, 1H, exocyclic vinylic-H), 6.07 (s, 1H, vinylic-_γ-pyrone), 4.65 (s, 2H, O–CH₂). ¹³C NMR (400 MHz, DMSO-d₆, δ, ppm): 186.02 (C=O), 180.48 (C=O), 162.21, 156.35, 149.35, 144.75, 141.42, 134.54, 131.2, 129.43, 127.21, 126.26, 125.75, 123.85, 121.54, 116.23, 114.62 (chroman/chromen ring), 66.43 (O–CH₂). MS (ES+) m/z: 382.

2.2.3. 2-Amino-3-(4'-oxo-chroman-3'-ylidene methyl)-chromen-4-one (6)

It was crystallized from CHCl₃–MeOH as cream color solid; Yield: 78%; m.p 203–05 °C. Anal. Calc. for C₁₉H₁₃NO₄: C, 71.47; H, 4.10; N, 4.39; found: C, 71.47; H, 4.11; N, 4.39; IR (KBr) cm⁻¹: 3304, 1664, 1615, 1410, 1314, 1214, 1154, 874. ¹H NMR (400 MHz, DMSO-d₆, δ, ppm): 9.75 (s, 2H, NH₂, D₂O exchangeable) 7.06–8.35 (m, 8H, Ar–H), 6.23 (s, 1H, exocyclic vinylic-H), 4.85 (s, 2H, O–CH₂). ¹³C NMR (400 MHz, DMSO-d₆, δ, ppm): 182.54 (C=O), 180.42 (C=O), 165.34, 158.23, 154.64, 135.86, 134.62, 131.43, 130.23, 129.54, 125.97, 123.32, 121.42, 120.73, 119.61, 115.29, 114.61, 102.43 (chroman/chromen ring), 68.94 (O–CH₂). MS (ES+) m/z: 319.

2.3. DNA binding experiments

2.3.1. Preparation of stock solution

The stock solution of DNA was prepared by dissolving DNA in Tris–HCL buffer (10 mM, pH 7.5) and compounds in a mixed solvent of 1% methanol and 99% Tris–HCL buffer. The purity of DNA was verified by monitoring the ratio of absorbance at 260 nm to that at 280 nm, which was in the range 1.8–1.9. The concentration of the DNA was determined spectrophotometrically using ε_{260nm} = 6600 M⁻¹ cm⁻¹ [32].

2.3.2. Absorbance spectroscopy

The UV–vis absorption of Calf thymus DNA was recorded on a 177 Beckman DU 40 Spectrophotometer (USA) by using a cuvette of 1 cm path length. The absorbance values of compounds (4–6) in the absence and presence of DNA were recorded in the range of 260–380 nm. The reference solution was the corresponding Tris–HCL buffer solution. While measuring the absorption spectra, equal amount of DNA was added to both the compounds solution and the reference solution to eliminate the absorbance of DNA itself.

2.3.3. Emission spectroscopy

To compare quantitatively the affinity of the compounds (4–6) with DNA, the binding constants *K* of the compounds binding to DNA were obtained by the fluorescence titration method. Fluorescence measurements were recorded on a Shimadzu 184 Spectrofluorimeter-5000 (Japan). The fluorescence quenching with increasing concentration of DNA was recorded after exciting the compounds (4–6) at 273 nm, using 10/10 nm as slit widths. Fixed

amounts of the compounds (10 μM) were titrated with increasing amounts of DNA.

2.3.4. Viscosity

To further elucidate the binding mode of compounds (**4–6**), viscosity measurements were carried out by keeping DNA concentration constant (50 μM) and varying the concentration of the compounds. Viscosity measurements were carried out with an Ubbelohde viscometer suspended vertically in a thermostat at 25 °C (accuracy ± 0.1 °C). The flow time was measured with a digital stopwatch, and each sample was tested three times to get an average calculated time. The data were presented as (η/η_0) versus concentrations of DNA/compound ratio, where η and η_0 are the viscosity of compounds in the presence and absence of DNA, respectively.

2.3.5. Molecular docking

The rigid molecular docking studies were performed by using HEX 6.1 software [33]. HEX is an interactive molecular graphics program for calculating and displaying feasible docking modes of DNA. The Hex 6.1 performs docking using Spherical Polar Fourier Correlations. It necessitates the ligand and the receptor as input in PDB format. The parameters used for docking include: correlation type – shape only, FFT mode – 3D, grid dimension – 0.6, receptor range – 180, ligand range – 180, twist range – 360, distance range – 40. The input is two molecules in PDB format and the output is a list of potential complexes sorted by shape complementary criteria. The crystal structure of the B-DNA dodecamer d(CGCGAATTCGCG)₂ (PDB ID: 1BNA) was downloaded from the protein data bank. The initial structures of the compounds (**4–6**) were generated by molecular modeling software Avagadro 1.01 using MMFF94 force field. Visualization of the docked pose has been done by using PyMol (<http://pymol.sourceforge.net/>) molecular graphic program [34].

2.4. Biological activity

The biological activity profile of the entire synthesized compound (**4–6**), as acetylcholinesterase (AChE) inhibitors, was assayed in comparison with tacrine as a reference compound. The retrieved protein (PDB: 2JEZ) used for this purpose was improved by using import and preparation option of MVD software and missing bond order, hybridization state, angle and flexibility for achieving reliable potential binding site in receptor. The energy minimized ligands (synthesized compounds) were drawn with Chem Draw Ultra (2D and 3D). Discovery studio 3.5 [35] and MVD [36] software were used to perform molecular docking, energy profile of ligand–receptor interaction independently.

2.4.1. In vitro acetylcholinesterase inhibition activity

The in vitro inhibition of AChE by the newly synthesized compounds (**4–6**) was screened spectrophotometrically by modified Ellman's coupled enzyme assay method using tacrine as reference [37]. Electric eel AChE (Type-VI-S, EC 3.1.1.7) was used as the enzyme sources while acetylthiocholine iodide as substrate and 5,5'-dithio-bis (2-nitrobenzoic) acid (DTNB) was also used in the anti-cholinesterase activity determination. In this procedure, the assay solution was composed of 0.1 mL of each sample (1 mg/mL in methanol), 0.02 mL of substrate (75 mM acetylthiocholine iodide in H₂O) and 0.1 mL of Ellman reagent (10 mM DTNB and 17.85 mM sodium bicarbonate in sodium phosphate buffer solution, pH 7.0). The reaction mixture was incubated for 15 min at 25 °C, 25 μL of enzyme solution containing 0.28U/mL (commercial acetylcholinesterase) was added to above mixture with 3.0 mL of sodium phosphate buffer and then further incubated for 5 min at 25 °C. The resulting solutions were placed in a spectrophotometer. For non-enzymatic reaction, the assays were carried out with a blank

containing all components except acetylcholinesterase. The difference of absorbance at 412 nm for sample and control was calculated as an inhibition rate (%). The percentage of enzyme inhibition was calculated using the following formula.

$$\% \text{ inhibition} = E - S/S \times 100$$

where E is the activity of the enzyme without test sample and S is the activity of enzyme with test sample. Tacrine was used as a standard inhibitor. The experiments were done in triplicate and the results were expressed as average values. An AChE inhibition activity of synthesized compounds is presented in Table 2.

3. Results and discussion

3.1. Chemistry

The protocol for the synthesis of compounds (**4–6**) is one step reaction methodology. To a stirred solution of 2,3-dihydro-1-benzopyran-4-one in absolute ethanol (25 mL) containing catalytic amount of piperidine, substituted 3-formyl chromones (**1–3**) were added. The reaction mixture was allowed to attain 140 °C temperature and was refluxed for 2–3 h. The structure elucidation of the synthesized compounds was confirmed from IR, ¹H NMR, ¹³C NMR and MS studies. The IR spectrum of the compounds (**4–6**) showed the characteristic peaks at 1664, 1651 and 1650 corresponding to cross conjugated (C=O) moiety, peaks at 1615, 1595 and 1591 corresponds to (C=C), moreover compound (**6**) exhibited a peak at 3304 cm⁻¹ corresponding to amine group. In ¹H NMR signals resonating at around 7.09–8.24, 7.15–8.11 and 7.06–8.35 integrating for 8, 7 and 8 protons is ascribed to aromatic protons of compounds **4**, **5** and **6** respectively. The sharp singlet signals resonating at 6.02, 6.13 and 6.23 is attributed to three exocyclic vinylic protons of compounds **4**, **5** and **6** respectively, this unexpected downfield shift of these protons is probably due to the H-bonding of these exocyclic vinylic protons with the adjacent carbonyl group. Signals resonating at 4.87, 4.65 and 4.85 each integrating for two protons, is assigned to –OCH₂ protons. Two singlets at 5.98 and 6.07 corresponds to vinylic proton of the γ -pyrone nucleus of the compounds **4** and **5** respectively.

The ¹³C NMR was also in agreement with the proposed structures. All the compounds exhibited carbonyl carbon (C=O) signal at 185.37, 183.24 (comp. **4**), 186.02, 180.48 (comp. **5**) and 182.54, 180.42 (compound **6**) respectively. A group of signals resonating around 135–114 is assigned to aromatic ring carbons, similarly signals appearing at 68.23, 66.43 and 68.94 corresponds to oxygenated methylene carbons (O–CH₂). Finally compounds (**4–6**) showed characteristic molecular ion peaks, MS (ES+) at m/z: 303, 382 and 319 respectively which were in good agreement with the proposed structures. The tentative mechanism, explaining the formation of products (**4–6**), has been proposed on the basis of spectral studies as shown in Scheme 2.

3.2. DNA binding studies

3.2.1. UV-absorption

UV-vis absorption is a very simple method and helps in depicting the structural changes and also sheds light on the complex formation [38–39]. The UV absorption spectrum (Fig. 1) shows the effect of DNA on the absorption spectrum of compounds (**4–6**). Absorption experiments were performed with fixed concentration of compounds (**4–6**) of 10 μM and gradually increasing the concentration of CT-DNA with the range from 5 to 30 μM . As seen in figure, the compounds (**4–6**) have strong absorption peaks at 274 nm and broad medium band at 273 nm. The binding of compounds (**4–6**) to DNA leads to decrease in the absorption intensities

Table 1
Binding parameters obtained from the fluorescence quenching method.

Compounds	$K_{sv} (1 \times 10^4)$ (M^{-1})	$K_q (1 \times 10^{12})$ ($M^{-1} s^{-1}$)	$K (1 \times 10^4)$ (M^{-1})	n	r^{2a}
4	1.38	1.38	0.64	1.03	0.996
5	1.17	1.17	1.35	0.92	0.996
6	2.07	2.07	2.97	1.01	0.994

^a r^2 is the regression in binding equilibria.

of the compounds (hypochromism), with a small amount of bathochromic shifts in the UV–vis absorption spectrum. Incorporation of compound within the base pairs of DNA, the π orbital of the compounds (**4–6**) can couple with the π orbital of the DNA base

pairs, thus, decreasing the $\pi \rightarrow \pi$ transition energy and resulting in the red shift. Such type of shift suggests an interaction between compounds (**4–6**) and DNA. In addition to this, the hypochromic effect is thought to be due to the increase in the interaction between the electronic states of the intercalating chromophore (compounds **4–6** and those of the DNA bases) [40]. As we know that the strength of this electronic interaction would decrease as the cube of the distance of separation between the chromophore and the DNA bases [41]. Hence, the large hypochromism observed in our systems suggested the close proximity of the compounds (**4–6**) to the DNA bases. Therefore UV–vis measurements suggest that the compounds (**4–6**) can interact with CT-DNA quite probably by intercalating into DNA base pairs.

Table 2
Quantitative estimation of acetylcholinesterase inhibition activity of compounds (**4–6**) by modified Ellaman's coupled enzyme assay method using Tacrine as reference ($n = 3$).

Entry	Compound	R_1	R_2	m.p (°C)	Yield (%)	Reaction time (h)	IC_{50} (μM) ^a AChE
1	4	H	H	145–147	84	2.5	1.23 ± 0.1
2	5	H	Br	188–190	73	2.3	0.96 ± 0.5
3	6	NH ₂	H	203–204	78	2.7	0.27 ± 0.3
Standard (Tacrine)							0.19 ± 0.03

^a IC_{50} : Concentration (means \pm SEM^a of three experiments) of compound for 50% inhibition of AChE, ^aSEM: Standard error of the mean.

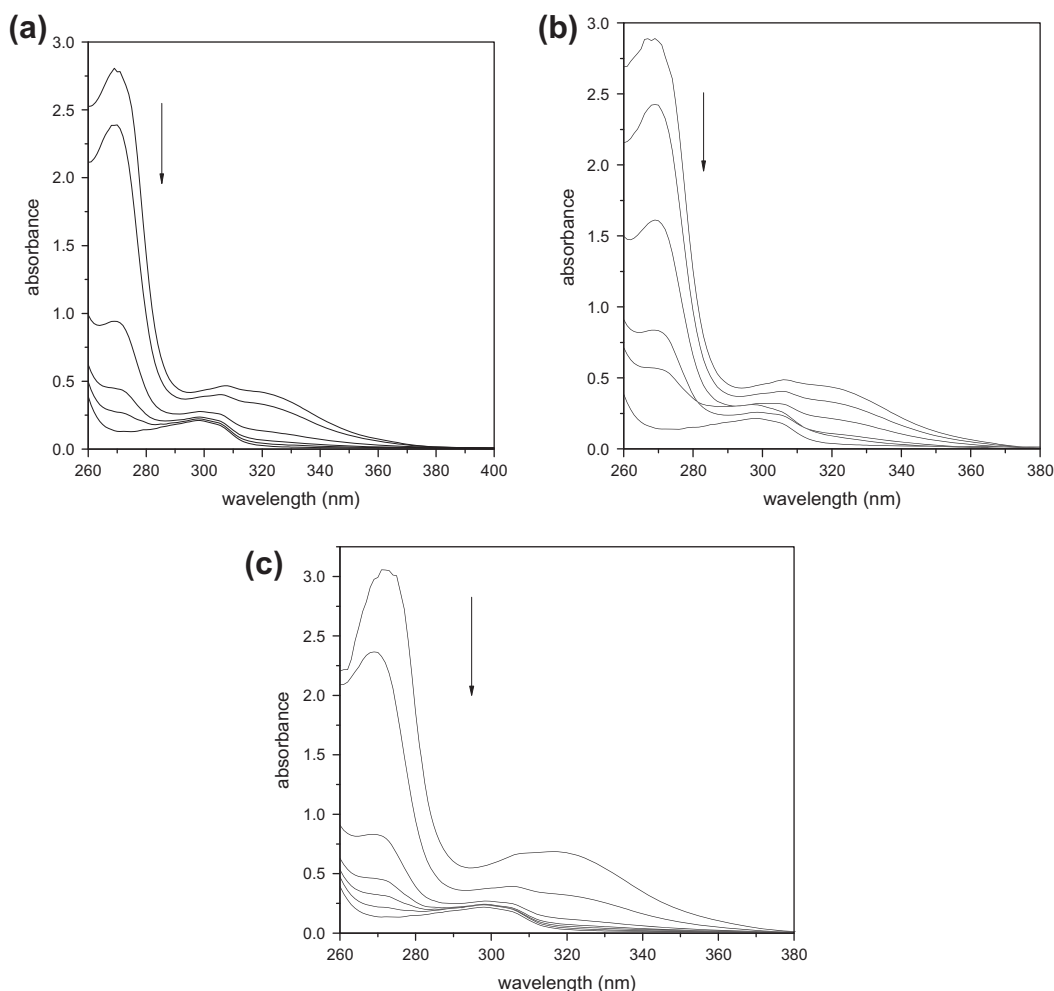


Fig. 1. Variation of UV–vis absorption spectra for compounds **4**(a), **5**(b) and **6**(c) with increase in the concentration of DNA. Arrow shows the absorbance changes upon increasing DNA concentration, [DNA = 0 to 25 μM]. Data represent mean \pm SD of three experiments. p value < 0.05 as compared to control.

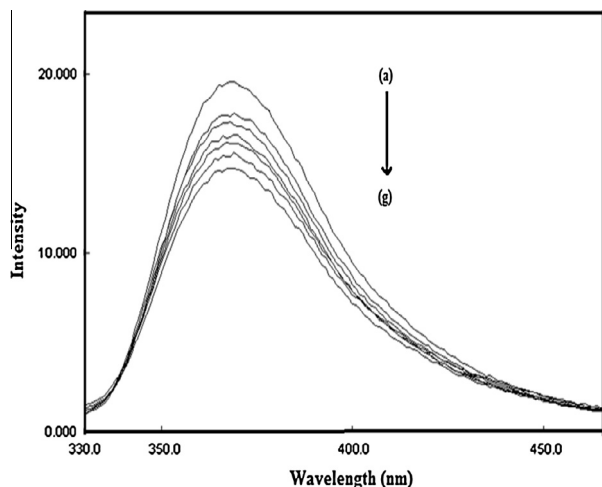


Fig. 2. The emission enhancement spectra of compound **4** (10 μM) in the presence of 0–20 μM DNA. Arrow shows the emission intensities upon increasing DNA concentration.

3.2.2. Fluorescence

Fluorescent quenching techniques involve a variety of molecular interactions such as excited state reactions, formation of ground-state complex, molecular rearrangements, energy transfer, and collision [42]. In this context, fluorescence quenching experiments were undertaken to investigate the interaction of synthesized compounds (**4–6**) with DNA. The binding of compounds (**4–6**) with DNA, by maintaining the concentration of compounds constant (i.e., 10 μM) and varying the concentration of DNA from 0 to 20 μM , was studied by fluorescence spectroscopy (Fig. 2). The fluorescence quenching data were analyzed to obtain the quenching constant by using the well-known Stern–Volmer equation [43].

$$\left(\frac{F_0}{F}\right) - 1 = k_{sv}[Q] \quad (1)$$

where F_0 and F denote the steady-state fluorescence intensities in the absence and in the presence of quencher (DNA), respectively, K_{SV} is the Stern–Volmer quenching constant (which is a measure of quenching efficiency), and $[Q]$ is the concentration of the quencher. Hence, Eq. (1) was applied to determine K_{SV} by linear regression of a plot of $(F_0/F) - 1$ versus concentration of DNA and is

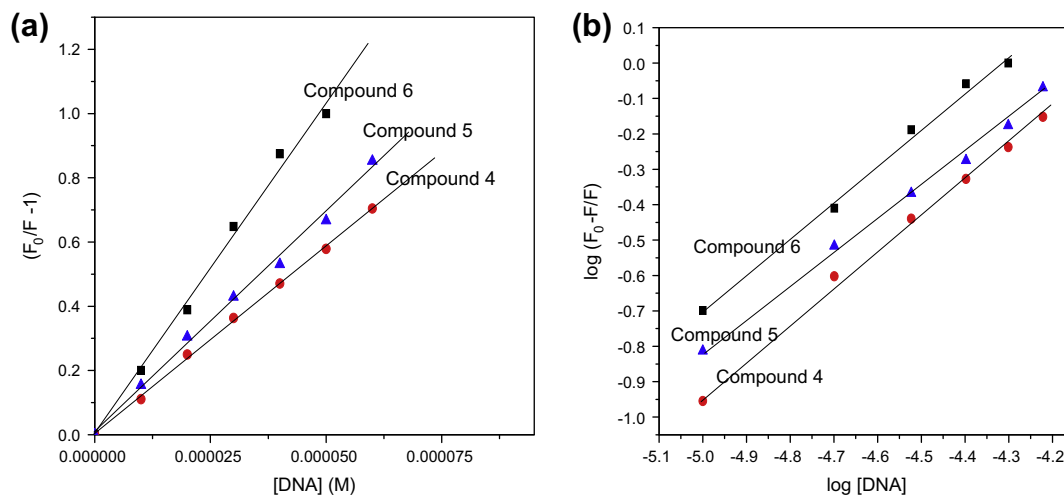


Fig. 3. (a) Stern–Volmer plots for the compounds (**4–6**). (b) Variation of $\log(F_0 - F)/F$ with \log concentration of DNA.

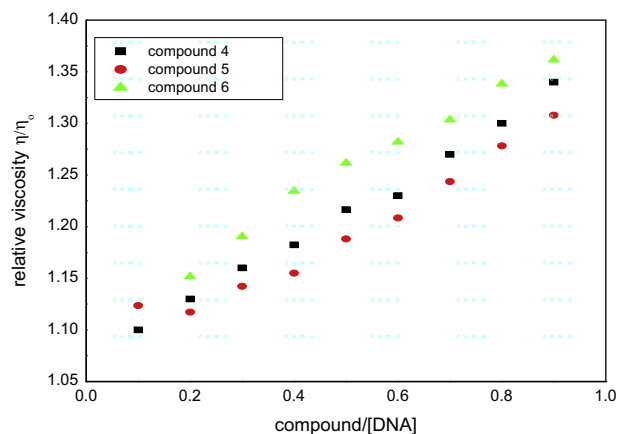


Fig. 4. Effect on relative viscosity of CT-DNA with an increase in concentration of the added compounds (**4–6**). Viscosity measurements were carried out with an Ubbelohde viscometer suspended vertically in a thermostat at 25 $^{\circ}\text{C}$ (accuracy ± 0.1 $^{\circ}\text{C}$).

represented in Fig 3a. The Stern–Volmer constants (K_{SV}) estimated for compounds (**4–6**) by Stern–Volmer equation were recorded in Table 1. The Stern–Volmer plot is linear, indicating that only one type of quenching process occurs, either static or dynamic.

Analysis of quenching mechanism was confirmed from the values of biomolecular quenching rate constants, which are evaluated by using the Eq. (2):

$$K_q = K_{sv}/\tau_0 \quad (2)$$

where K_q is the quenching rate constant of the biomolecules and τ_0 is the lifetime of the biomolecules without the quencher ($\tau_0 = 10^{-8}$ s of various biopolymers) [44]. For dynamic quenching, the maximum scatter collision constant of various quenchers was $2 \times 10^{10} \text{ M}^{-1} \text{ s}^{-1}$. The values of K_q were much greater than $2 \times 10^{10} \text{ M}^{-1} \text{ s}^{-1}$ (Table 1), which depicts that probable interaction of compounds (**4–6**) with DNA, was initiated by a static quenching process i.e., formation of a complex. For static quenching, the relationship between fluorescence intensity and concentration of a quencher can be described by the equation shown below [45]:

$$\log \frac{F_0 - F}{F} = \log K + n \log [Q]$$

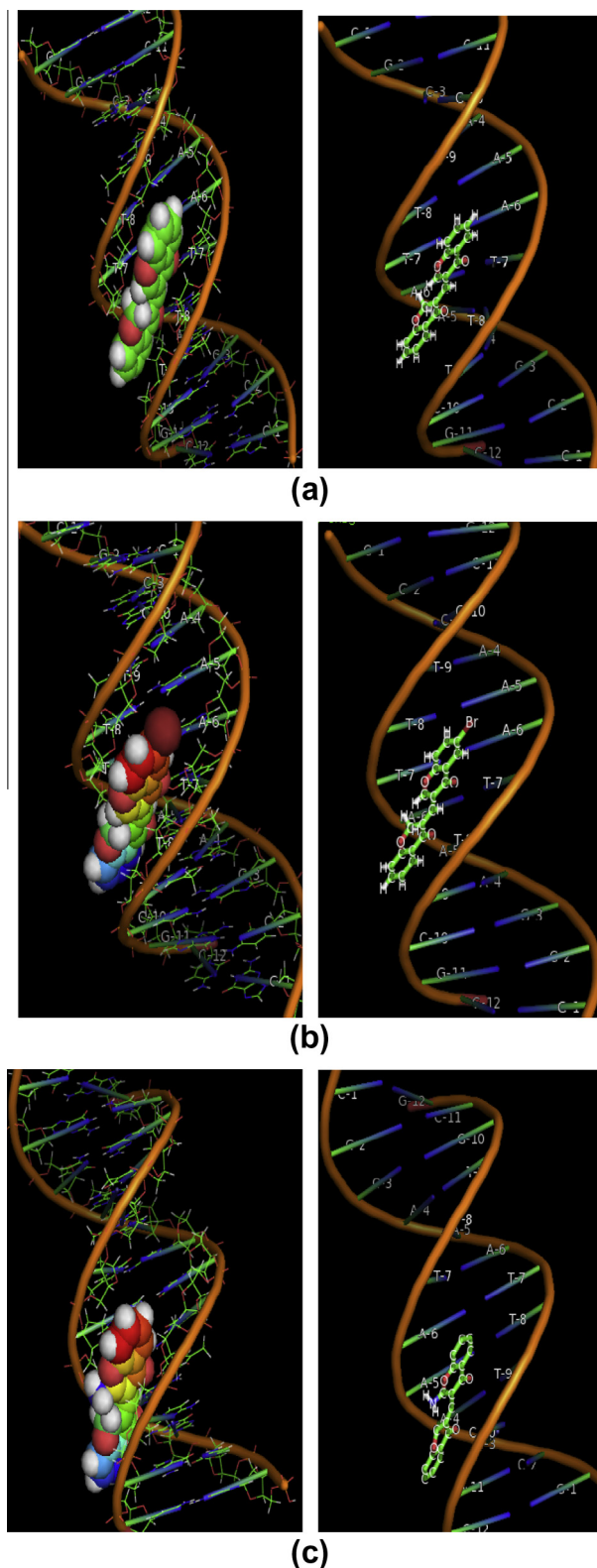


Fig. 5. Cartoon representation of DNA with bound compounds. (a)–(c) shows minimum energy poses of DNA–compound **4**, DNA–compound **5** and DNA–compound **6** complexes respectively. Each panel contains two figures, which show solid and stick representation of compounds. In stick model of compound **6** (c), the hydrogens attached to carbons are removed, in order to have easy visualization of amino hydrogen inclined towards A5 of the DNA strand.

where K and n are the binding constant and the number of binding sites, respectively. From the plot of $\log(F_0 - F)/F$ vs. $\log[Q]$, K and n values can be obtained from the intercept and slope (Fig. 3b). The

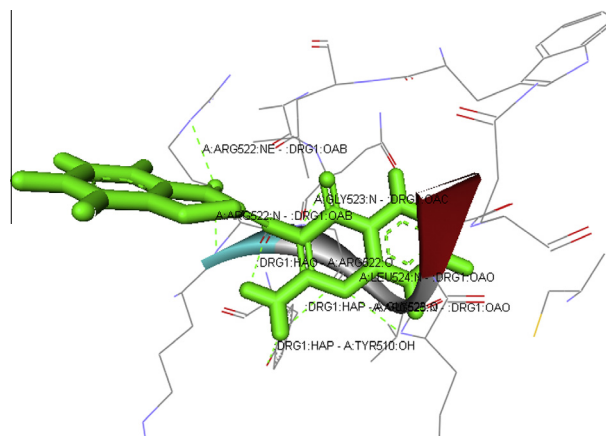


Fig. 6. Docking model of compound **6** interacting with amino acid residues in the binding site of protein (PDB: 2JEZ). The available binding sites for compound **6** are A:ARG522:N-DRG1:OAB, A:ARG522:NE:DRG1:OAB, A:GLY523:N-DRG1:OAC, A:LEU524:N-DRG1:OAO, A:ARG525:N-DRG1:OAO, DRG1:HAO - A:ARG522:O, DRG1:HAP - A:TYR510:OH, DRG1:HAP - A:GLY523:O. The compound is shown in green stick model. Pictures are created with Discover Studio 3.5. (For interpretation of the references to color in this figure legend, the reader is referred to the web version of this article.)

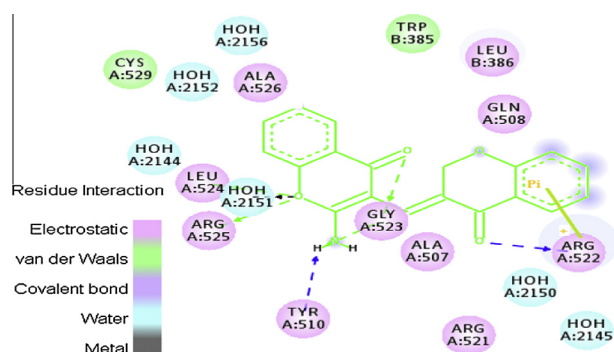
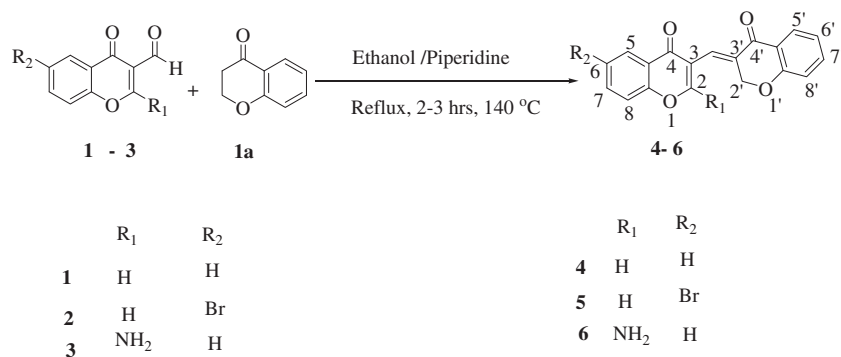
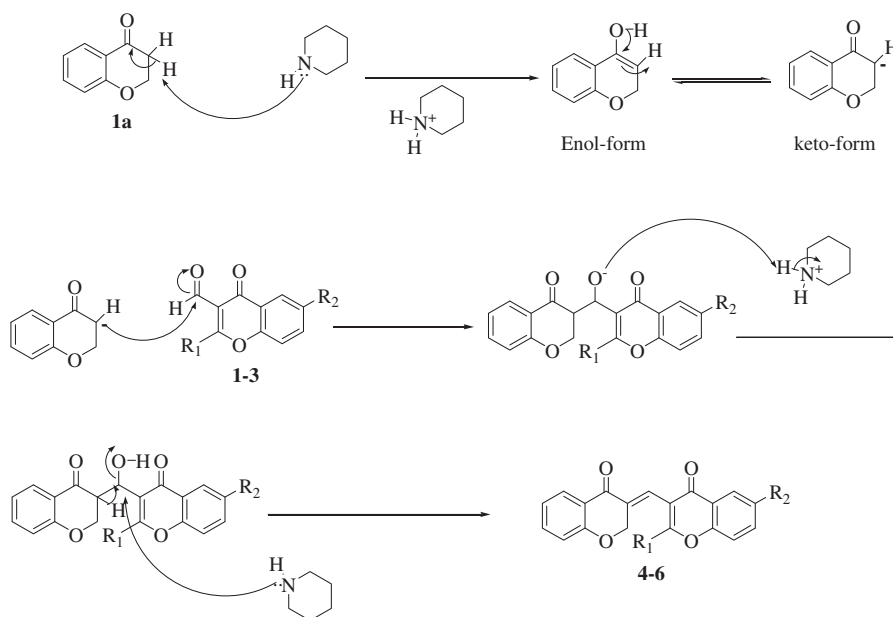


Fig. 7. Ligand (compound **6**) displaying various interactions with amino acid residues at active sites of the protein (PDB: 2JEZ) along with pi-cation interaction with amino acid residue ARG 522.

values of n were approximately equal to **1**, which suggests the existence of just one binding site on DNA for compounds (**4**–**6**). The value of K is significant, in order to quantify the interaction between compounds (**4**–**6**) and DNA. The larger values of the K observed in the present study depicts the stronger interaction between the compounds (**4**–**6**) and DNA. Earlier Wang et al. [46], proposes the intercalative mechanism between the 6-ethoxy chromone-3-carbaldehyde benzoyl hydrazone and DNA, with a binding constant of $8.27 \times 10^5 \text{ M}^{-1}$. Yong. Li et al. [47], reported the binding of 3-carbaldehyde chromone-(benzoyl) hydrazone with DNA through intercalative mechanism and the binding constant reported is $7.39 \times 10^5 \text{ M}^{-1}$. By comparing these literature values with our data, the binding constant in our system are slightly towards lower side, but these values are too higher than surface binding of compounds with DNA. Nafisi et al. [48], reported the intercalative and external binding mechanism for various fluorescent probes with CT-DNA and their binding constants vary from $(6.58\text{--}2.13) \times 10^4 \text{ M}^{-1}$. Hence, it may be proposed that compounds (**4**–**6**) interact with DNA in an intermediate way between the surface binding at one end and intercalative at the other (i.e., partially intercalated, discussed in next section). The data shown in (Table 1) also suggests that the interaction of the compounds (**4**–**6**) with DNA follows the order: compound **6** > compound **5** > compound **4**. This variation likely reflects the differing ability of these ligands to stack and overlap well with the base pairs of DNA.



Scheme 1. Synthesis of 3-formyl chromone derivatives (**4-6**).



Scheme 2. Plausible mechanism for the synthesis of compounds (**4-6**) via Knoevenagel Condensation of 4-chromanone (**1a**) and substituted 3-formyl chromones (**1-3**) catalyzed by piperidine.

3.2.3. Viscosity results

The binding modes of the compounds (**4-6**) with CT-DNA, was further confirmed by viscosity measurements. In case of classical intercalation binding, a ligand must lengthen the DNA helix due to the separation of base pairs, resulting in increased viscosity of DNA. On the other hand, if the drug is groove binder or interacts electrostatically with DNA, the viscosity of solution does not change significantly [49,50]. From Fig. 4, it is clearly evident that the presence of compounds had an obvious effect on relative viscosity of CT-DNA with an increase in concentration of the added compounds. These results demonstrate that compounds (**4-6**) bind to DNA through the intercalation mode.

3.2.4. DNA-binding docking studies

Molecular docking is a powerful tool for the design of ligands toward a specific biopolymer target. Molecular docking is commonly used in the field of drug design to predict the binding of small molecules to biological protein targets. This method gives the possibility to study an active site in detail and can be used for hit identification, virtual screening and binding mode determination. In our experiment, rigid molecular docking (two interacting molecules were treated as rigid bodies) studies were performed to predict the binding modes of compounds (**4-6**) with a DNA duplex

of sequence d (CGCAAATTCGC)₂ dodecamer (PDB ID: 1BNA), and provide an energetically favorable docked structures (representative figure of DNA-compounds (**4-6**) complex shown in Fig. 5). It is apparent from the Fig. 5, that the chromone moiety in compounds (**4-6**) find its position within the base pairs of DNA (intercalation) and the chroman part of compounds (**4-6**) remain in the minor groove region of DNA. In this configuration, the amino group in compound **6** and bromo group in compound **5** remains inclined towards the DA5 of strand A of the DNA double helix. This observation suggests that compounds (**4-6**) interact with DNA through minor groove binding and partial intercalation. Partial intercalation is the preferred mode of interaction for the compounds, where the two biphenyl rings are connected by unfused biphenyl linkage. In the same context, compounds (**4-6**) contains two rings connected by fused =CH— linkage, hence interacts with DNA in partial intercalative manner. Amutha et al. [51], have suggested partial intercalative mechanism in case of benzidine (where two pheny rings are connected by biphenyl linkage) with binding constant of $6.7 \times 10^3 \text{ M}^{-1}$. The resulting relative binding energy of docked chromone–DNA complexes was found to be $212.10 \text{ kJ mole}^{-1}$ (compound **4**), $235.23 \text{ kJ mole}^{-1}$ (compound **5**) and $242.11 \text{ kJ mole}^{-1}$ (compound **6**). High values of binding energy in case of compound **6** and **5**, depicts the role of hydrogen bonding

between these substituent's with nitrogen base pairs of DNA [52]. These values are in agreement with the high binding constants obtained from spectrofluorimetry. Hence, we can conclude that there is a mutual complement between molecular modeling and fluorescence quenching, which provide valuable information about the mode of interaction of the compounds (4–6) with DNA.

3.2.5. Acetylcholinesterase Inhibition docking studies

The acetylcholinesterase inhibition data (Table 2) obtained is further investigated on structural basis, molecular modeling and docking studies. With the aim to understand the ligand–protein interactions, molecular docking studies were performed for the most potent AChE inhibitor reported in this work (compound 6), a molecular modeling study was performed using the docking program Discovery Studio 3.5. The docking studies illustrate that compound 6 has several interactions along the active-site gorge of AChE as shown in Figs. 6 and 7. Discovery software was performed in order to predict the affinity and orientation of the synthesized compound 6 at the active site. The hydrogen bonds formed with amino acids of the protein showed good agreement with the predicted binding affinities obtained by molecular docking studies as verified by acetylcholinesterase inhibition activity data where compound 6 was found to be most potent AChE inhibitor ($IC_{50} = 0.27$). The improved activity of the compound 6 in comparison to compounds 4 and 5, can be explained on the basis of its skeleton, that the presence of amine group at C-2 of benzo- γ -pyrone ring of compound 6, increases activity due to the formation of additional hydrogen bonds with amino acid residues TYR 510 and GLY 523 of the protein and easily perform as guest relation with receptor protein (host) (Figs. 6 and 7). Compounds 4 and 5 showed moderate profile of AChE inhibition. The acetylcholinesterase inhibition potency of compounds was seen in the order: Compound 6 > compound 5 > compound 4. It has been previously reported that halogenated compounds show acetylcholinesterase inhibition activity [53]. In the same context, it can be inferred from the data, that Compound 5 ($IC_{50} = 0.96$) showed better inhibition activity against AChE as compared to compound 4 ($IC_{50} = 1.23$), probably due to the presence of halogen (Br) at C-6 of the benzo- γ -pyrone ring. In addition, the proposed active inhibitor (compound 6), simulates the residual interaction with the respective amino acid residues like ARG 522, LEU 524 and ARG 525, through carbonyl and pyrone ring oxygen atoms (Fig. 7). Moreover benzene ring of the chroman moiety in compound 6 played a major role in stabilizing the ligand–receptor complex by pi-cation interactions with amino acid residue ARG 522 shown in Fig 7. Hence, the proposed compounds 6 can be used for further scientific studies and can be extended to experimental validation.

4. Conclusion

The present study reports the synthesis of substituted 3-formyl chromone derivatives (4–6) by Knoevenagel Condensation, structurally correlated to known bisintercalators. The detailed fluorescence spectra, electronic absorption spectra and molecular docking studies undertaken in the present work are in total agreement, with the primary partial intercalative mode of binding, although the van der Waals and other types of interactions can also be argued. DNA-binding constant of compound (6) was found to be ($2.97 \times 10^4 M^{-1}$) higher than compounds (4) and (5). All the synthesized compounds were tested for AChE inhibition activity, compound (6) was found to be promising candidate, further verified by docking studies. Information obtained from the results, suggest that these synthesized chromone derivatives can be used as templates for future research, for designing new entities through

modification and derivatization with an improved DNA binding and AChE inhibition affinities for therapeutic purposes.

Acknowledgments

One of the authors A. Mohammed thanks the chairman, Department of Chemistry, A.M.U, Aligarh for providing necessary research facilities and acknowledges UGC for financial support. The CSIR, New Delhi, is also thanked for the award of Research Associateship to M. Alam.

References

- [1] G.P. Ellis, Chromenes, chromanones, and chromones, In the Chemistry of Heterocyclic Compounds, vol. 31, Wiley, New York, 1977.
- [2] V. Ya Sosnovskikh, Synthesis and reactions of halogen-containing chromones, Russ. Chem. Rev. 72 (2003) 489–516.
- [3] J.A. Manthy, B.S. Buslig (Eds.), Flavonoids in the Living Systems: Advances in Experimental Medicine and Biology, vol. 439, Plenum, New York, 1998.
- [4] C. Hansch, P.G. Sammes, J.B. Taylor (Eds.), Comprehensive Medicinal Chemistry, vol. 6, Pergamon, New York, 1990.
- [5] G.P. Ellis (Ed.), The Chemistry of Heterocyclic Compounds, Chromenes, Chromanones and Chromones, vol. 31, J. Wiley & Sons, New York, 2007.
- [6] (a) M.P.S. Ishar, G. Singh, S. Singh, K.K. Sreenivasan, G. Singh, Synthesis and evaluation of novel 6-chloro-fluorochromone derivatives as potential topoisomerase inhibitor anticancer agents, Bioorg. Med. Chem. Lett. 16 (2006) 1366–1370; (b) S. Alcaro, A. Gaspar, F. Ortuso, N. Milhazes, F. Orallo, E. Uriarte, M. Yanez, F. Borges, Chromone-2- and -3-carboxylic acids inhibit differently monoamine oxidases A and B, Bioorg. Med. Chem. Lett. 20 (2010) 2709–2712; N. Desideri, A. Bolasco, R. Fioravanti, L. Proietti Monaco, F. Orallo, M. Yanez, F. Ortuso, S. Alcaro, Homoisoflavonoids: natural scaffolds with potent and selective monoamine oxidase-B inhibition properties, J. Med. Chem. 54 (2011) 2155–2164.
- [7] A. Gaspar, J. Reis, A. Fonseca, N. Milhazes, D. Vina, E. Uriarte, M.F. Borges, Chromone 3-phenylcarboxamides as potent and selective MAO-B inhibitors, Bioorg. Med. Chem. Lett. 21 (2011) 707–709.
- [8] (a) C.K. Ghosh, Chemistry of 4-Oxo-4H-[1]benzopyran-3-carboxaldehyde, J. Heterocycl. Chem. 20 (1983) 1437–1445; (b) C.K. Ghosh, A. Patra, Chemistry and application of 4-oxo-4H-1-benzopyran-3-carboxaldehyde, J. Heterocycl. Chem. 45 (2008) 1529–1547.
- [9] H. Lee, K. Lee, J.K. Jung, J. Cho, E.A. Theodorakis, Synthesis and evaluation of 6-hydroxy-7-methoxy-4chromanone-and chroman-2-carboxamides as antioxidants, Bioorg. Med. Chem. Lett. 15 (2005) 2745–2748.
- [10] D.L. Yu, M. Suzuki, L. Xie, S.L. Morris-Natschke, K.H. Lee, Recent progress in the development of coumarin derivatives as potent anti-HIV agents, Med. Res. Rev. 23 (2003) 322–345.
- [11] I.M. Chandler, C.R. Mcintyre, T.J. Simpson, Structural revision and synthesis of LI-D253-alpha and related chromanone fungal metabolites, J. Chem. Soc. Perkin Trans. 1 (18) (1992) 2271–2284.
- [12] C. Dyrager, L.N. Mollers, L.K. Kjall, J.P. Alao, P. Diner, F.K. Wallner, P. Sunnerhagen, M. Grotli, Design, synthesis, and biological evaluation of chromone-based p38 MAP kinase inhibitors, J. Med. Chem. 54 (2011) 7427–7431.
- [13] M.E. Welsch, S.A. Snyder, B.R. Stockwell, Privileged scaffolds for library design and drug discovery, Curr. Op. Chem. Biol. 14 (2010) 347–361.
- [14] V.Y. Sosnovskikh, V.S. Moshkin, M.I. Kodess, A reinvestigation of the reactions of 3-substituted chromones with hydroxylamine. Unexpected synthesis of 3-amino-4H-chromeno[3,4-d]isoxazol-4-one and 3-(diaminomethylene) chroman-2,4-dione, Tetrahedron Lett. 49 (2008) 6856–6859.
- [15] V.Y. Sosnovskikh, V.S. Moshkin, M.I. Kodess, Reactions of 3-(polyfluoroacyl) chromones with hydroxylamine: synthesis of novel RF-containing isoxazole and chromone derivatives, Tetrahedron 64 (2008) 7877–7889.
- [16] V.Y. Sosnovskikh, R.A. Irgashev, V.S. Moshkin, M.I. Kodess, Reaction of 3-(polyfluoroacyl)chromones with hydrazines: new regioselective synthesis of RF-containing pyrazoles, Russ. Chem. Bull. Int. Ed. 57 (2008) 2146–2155.
- [17] K. Enander, L. Choulier, A.L. Olsson, D.A. Yushchenko, D. Kanmert, A.S. Klymchenko, A.P. Demchenko, Y. Mely, D. Altschuh, A peptide-based, ratiometric biosensor construct for direct fluorescence detection of a protein analyte, Bioconjugate Chem. 19 (2008) 1864–1870.
- [18] V.V. Shynkar, A.S. Klymchenko, E. Piemont, A.P. Demchenko, Y. Mely, Dynamics of intermolecular hydrogen bonds in the excited states of 4'-dialkylamino-3-hydroxyflavones. On the pathway to an ideal fluorescent hydrogen bonding sensor, J. Phys. Chem. A 108 (2004) 8151–8159.
- [19] G. M'Baye, V.V. Shynkar, A.S. Klymchenko, Y. Mely, G. Duportail, Membrane dipole potential as measured by ratiometric 3-hydroxyflavone fluorescence probes: accounting for hydration effects, J. Fluoresc. 16 (2006) 35–42.
- [20] A.S. Klymchenko, G. Duportail, T. Ozturk, V.G. Pivovarenko, Y. Mely, A.P. Demchenko, Novel two-band ratiometric fluorescence probes with different location and orientation in phospholipid membranes, Chem. Biol. 9 (2002) 1199–1208.

- [21] A.S. Klymchenko, V.V. Shvadchak, D.A. Yushchenko, N. Jain, Y. Mely, Excited-state intramolecular proton transfer distinguishes microenvironments in single and double-stranded DNA, *J. Phys. Chem. B* 112 (2008) 12050–12055.
- [22] J. Wang, X.Y. Yi, B.D. Wang, Z.Y. Yang, DNA-binding properties studies and spectra of a novel fluorescent Zn(II) complex with a new chromone derivative, *J. Photochem. Photobiol., A* 201 (2009) 183–190.
- [23] R. Torkin, J.F. Lavoie, D.R. Kaplan, H. Yeger, Induction of caspase-dependent, p53-mediated apoptosis by apigenin in human neuroblastoma, *Mol. Cancer Ther.* 4 (2005) 1–11.
- [24] Y. Jin, J.A. Cowan, DNA cleavage by copper-ATCUN complexes. Factors influencing cleavage mechanism and linearization of dsDNA, *J. Am. Chem. Soc.* 127 (2005) 8408–8415.
- [25] K.E. Erkkila, D.T. Odom, J.K. Barton, Recognition and reaction of metallointercalators with DNA, *Chem. Rev.* 99 (1999) 2777–2796.
- [26] J. Smith, K. Ariga, E.V. Anslyn, Enhanced imidazole-catalyzed RNA cleavage induced by a bis-alkylguanidinium receptor, *J. Am. Chem. Soc.* 115 (1993) 362–364.
- [27] J.R. Morrow, L.A. Buttrey, V.M. Shelton, K.A. Berback, Efficient catalytic cleavage of RNA by lanthanide(III) macrocyclic complexes: toward synthetic nucleases for *in vivo* applications, *J. Am. Chem. Soc.* 114 (1992) 1903–1905.
- [28] M.S. Muche, M.W. Gobel, Bis(guanidinium) alcohols as models of staphylococcal nuclease: substrate binding through ion pair complexes and fast phosphoryl transfer reactions, *Angew. Chem. Int. Ed.* 35 (1996) 2126–2129.
- [29] U. Scheffer, A. Strick, V. Ludwig, S. Peter, E. Kalden, M.W. Gobel, Metal-Free catalysts for the hydrolysis of RNA derived from guanidines, 2-aminopyridines, and 2-aminobenzimidazoles, *J. Am. Chem. Soc.* 127 (2005) 2211–2217.
- [30] M.F. Brana, M. Cacho, A. Gradillas, B. de Pascual-Teresa, A. Ramos, Intercalators as anticancer drugs, *Curr. Pharm. Des.* 7 (2001) 1745–1780.
- [31] M.F. Brana, M. Cacho, A. Ramos, M.T. Dominguez, J.M. Pozuelo, C. Abradelo, M.F. Rey-Stolle, M. Yuste, C. Carrasco, C. Bailly, Synthesis, biological evaluation and DNA binding properties of novel mono and bisnaphthalimides, *Org. Biomol. Chem.* 1 (2003) 648–654.
- [32] G.S. Son, J.-Ah Yeo, M.-Sun Kim, S.K. Kim, A. Holmen, B. Akerman, B. Norden, Binding mode of norfloxacin to calf thymus DNA, *J. Am. Chem. Soc.* 120 (1998) 6451–6457.
- [33] D. Mustard, D.W. Ritchie, Docking essential dynamics eigenstructures, *Struct. Funct. Bioinf.* 60 (2005) 269–274.
- [34] W.L. DeLano, The PyMOL Molecular Graphics System, DeLano Scientific, San Carlos, CA, USA, 2002.
- [35] Accelrys software inc., Discovery Studio Modeling Environment, Release 3.1., 2011.
- [36] R. Thomsen, M.H. Christensen, MolDock: a new technique for high-accuracy molecular docking, *J. Med. Chem.* 11 (2006) 3315–3321.
- [37] G.L. Ellman, K.D. Courtney, V.J. Andres, R.M. Feather-Stone, A new and rapid colorimetric determination of acetylcholinesterase activity, *Biochem. Pharmacol.* 7 (1961) 88–90.
- [38] S.Y. Bi, D.Q. Song, Y. Tian, X. Zhou, Z.Y. Liu, H.Q. Zhang, Molecular spectroscopic study on the interaction of tetracyclines with serum albumins, *Spectrochim. Acta, Part A* 61 (2005) 629–636.
- [39] P.B. Kandagal, S. Ashoka, J. Seetharamappa, V. Vanb, S.M.T. Shaikh, Study of the interaction between doxepin and human serum albumins by spectroscopic methods, *J. Photochem. Photobiol., A* 179 (2006) 161–166.
- [40] R. Fukuda, S. Takenaka, M. Takagi, Metal ion assisted DNA interaction of crown ether-linked acridine derivatives, *J. Chem. Soc., Chem. Commun.* (1990) 1028–1030.
- [41] C. Cantor, P.R. Schimmel, The conformation of biological macromolecules, biophysical chemistry, W.H. Freeman, San Francisco, CA, 1980. p. 287.
- [42] M.R. Eftink, Fluorescence Quenching Reaction: Probing Biological Macromolecular Structures, Biophysical and Biochemical Aspects of Fluorescence Spectroscopy, Plenum Press, New York, 1991.
- [43] J.R. Lakowicz, Principles of Fluorescence Spectroscopy, Plenum Press, New York, 1983.
- [44] D.M. Togashi, A.G. Ryder, A fluorescence analysis of ANS bound to bovine serum albumin: binding properties revisited by using energy transfer, *J. Fluoresc.* 18 (2008) 519–526.
- [45] J. Min, X. Meng-Xia, Z. Dong, L. Yuan, L. Xiao-Yu, C. Xing, Spectroscopic studies on the interaction of cinnamic acid and its hydroxyl derivatives with human serum albumin, *J. Mol. Struct.* 692 (2004) 71–80.
- [46] J. Wang, Z.-Y. Yang, X.-Y. Yi, B.-D. Wang, DNA-binding properties studies and spectra of a novel fluorescent Zn(II) complex with a new chromone derivative, *J. Photochem. Photobiol. A Chem.* 201 (2009) 183–190.
- [47] Y. Li, Z.-Y. Yang, Rare earth complexes with 3-carbaldehyde chromone-(Benzoyl) hydrazone: synthesis, characterization, DNA binding studies and antioxidant activity, *J. Fluoresc.* 20 (2010) 329–342.
- [48] S. Nafisi, A.A. Saboury, N. Keramat, J.-F. Neault, H.-A. Tajmir-Riahi, Stability and structural features of DNA intercalation with ethidium bromide, acridine orange and methylene blue, *J. Mol. Struct.* 827 (2007) 35–43.
- [49] I. Haq, P. Lincoln, D. Suh, B. Norden, B.Z. Chowdhry, J.B. Chaires, Interaction of Δ - and λ -[Ru(phen)₂DPPZ]²⁺ with DNA: a calorimetric and equilibrium binding study, *J. Am. Chem. Soc.* 117 (1995) 4788–4796.
- [50] S. Satyanarayana, J.C. Dabrowiak, J.B. Chaires, Neither Δ - nor λ -Tris(phenanthroline)ruthenium(II) binds to DNA by classical intercalation, *Biochemistry* 31 (1992) 9319–9324.
- [51] R. Amutha, V. Sbramanian, B.U. Nair, Interaction of benzidine with DNA: experimental and modelling studies, *Chem. Phys. Lett.* 344 (2001) 40–48.
- [52] M.A. Husain, Z. Yaseen, S.U. Rehman, T. Sarwar, M. Tabish, Naproxen intercalates and causes photocleavage of DNA through ROS generation, *FEBS J.*, DOI:10.1111/febs.12558.
- [53] U. Brodbeck, K. Schweikert, R. Gentinetta, M. Rottenberg, Fluorinated aldehydes and ketones acting as quasi-substrate inhibitors of acetylcholinesterase, *Biochim. et Biophys. Acta (BBA)-Enzymol.* 567 (1979) 357–369.